ORIGINAL ARTICLE

CrossMark

Investigation of brain structure in the 1-month infant

Douglas C. Dean III[1,2] · E. M. Planalp[1,3] · W. Wooten[2] · C. K. Schmidt[1,2] · S. R. Kecskemeti[1] · C. Frye[2] · N. L. Schmidt[1,2] · H. H. Goldsmith[1,3] · A. L. Alexander[1,4,5] · R. J. Davidson[1,2,3,4]

Abstract

The developing brain undergoes systematic changes that occur at successive stages of maturation. Deviations from the typical neurodevelopmental trajectory are hypothesized to underlie many early childhood disorders; thus, characterizing the earliest patterns of normative brain development is essential. Recent neuroimaging research provides insight into brain structure during late childhood and adolescence; however, few studies have examined the infant brain, particularly in infants under 3 months of age. Using high-resolution structural MRI, we measured subcortical gray and white matter brain volumes in a cohort ($N = 143$) of 1-month infants and examined characteristics of these volumetric measures throughout this early period of neurodevelopment. We show that brain volumes undergo age-related changes during the first month of life, with the corresponding patterns of regional asymmetry and sexual dimorphism. Specifically, males have larger total brain volume and volumes differ by sex in regionally specific brain regions, after correcting for total brain volume. Consistent with findings from studies of later childhood and adolescence, subcortical regions appear more rightward asymmetric. Neither sex differences nor regional asymmetries changed with gestation-corrected age. Our results complement a growing body of work investigating the earliest neurobiological changes associated with development and suggest that asymmetry and sexual dimorphism are present at birth.

Keywords Magnetic resonance imaging · Brain volume · Sexual dimorphism · Brain asymmetry

✉ Douglas C. Dean III
deaniii@wisc.edu

1 Waisman Center, University of Wisconsin-Madison, Madison, WI 53705, USA

2 Center for Healthy Minds, University of Wisconsin-Madison, Madison, WI, USA

3 Department of Psychology, University of Wisconsin-Madison, Madison, WI, USA

4 Department of Psychiatry, University of Wisconsin-Madison School of Medicine and Public Health, Madison, WI, USA

5 Department of Medical Physics, University of Wisconsin-Madison School of Medicine and Public Health, Madison, WI, USA

Introduction

Human brain development is a complex but fundamental process necessary for the establishment of cognitive and behavioral function. Initiated in utero, neurodevelopmental processes such as neuronal pruning, synaptogenesis, and myelination operate under the direction of genetic and environmental forces to shape neural architecture and its underlying circuitry (Stiles and Jernigan 2010; Kolb and Gibb 2011). Although these processes continue across the lifespan, the time immediately following birth corresponds with a period of rapid brain development that provides the foundation for the earliest cognitive and behavioral skills. Moreover, the brain is most malleable and likely vulnerable to early experiences and insults during this developmental period (Dobbing 1990; Andersen 2003). For instance, neurodevelopmental and psychiatric disorders, such as autism spectrum disorders (Belmonte et al. 2004; Courchesne and Pierce 2005; DiCicco-Bloom et al. 2006), likely manifest during the first years of life as a result of alterations in early brain development. However, how these early alterations

🖄 Springer

occur and what is impacted by potentially adverse neurodevelopmental mechanisms is unknown. Thus, to effectively identify possible neurobiological substrates of early emerging psychological disorder, it is critical to understand early normative brain development.

Magnetic resonance imaging (MRI) affords the ability to non-invasively examine the structural and functional organization of the brain and provides key insight into the complex changes that take place during neurodevelopment. Although the majority of neuroimaging studies of brain development have been conducted in children beyond the age of 4 years (Pfefferbaum et al. 1994; Giedd et al. 1996, 1999; Caviness et al. 1996; Gogtay et al. 2004; Evans et al., 2006; Gogtay and Thompson 2010; Giedd and Rapoport 2010) due to the inherent challenge of acquiring MRI data in younger infants and toddlers, recent studies have begun to fill this knowledge gap (Hüppi et al. 1998a; Courchesne et al. 2000; Paus et al. 2001; Gilmore et al. 2007, 2012; Knickmeyer et al. 2008; Deoni et al. 2012; Dean et al. 2014c; Dubois et al. 2014; Holland et al. 2014; Makropoulos et al. 2016; Makki and Hagmann 2017). Still, few of these studies have examined structural relations in the brain of infants younger than 3 months of age. Huppi et al. compared quantitative volumetric brain measures between premature and mature neonates and found pronounced increases in gray and white matter volume throughout the perinatal period (Hüppi et al. 1998b). Gilmore et al. observed cortical gray matter growth in the first few weeks following birth, while in a follow-up longitudinal analysis, cortical and subcortical gray maturation strongly developed within the first year of life (Knickmeyer et al. 2008; Gilmore et al. 2012). More recently, Makropoulos et al. assessed regional brain growth in a large-scale database of preterm and term neonates, finding both absolute and relative brain volumes to significantly increase with age as well as distinct developmental differences between preterm and term infants (Makropoulos et al. 2016). White matter, on the other hand, initially develops at a slower rate (Knickmeyer et al. 2008), before developing exponentially during later infancy and childhood (Mukherjee et al. 2001, 2002; Deoni et al. 2012; Dean et al. 2014c, 2016; Dubois et al. 2014).

Hemispheric asymmetry exists across structural and functional levels of the adult brain (Toga and Thompson 2003; Hugdahl and Davidson 2004). Such asymmetry is also found during the prenatal period (Dehaene-Lambertz et al. 2006), but asymmetry patterns differ once infants reach full term (Gilmore et al. 2007). Moreover, white matter asymmetry is apparent across childhood (O'Muircheartaigh et al. 2013), suggesting that asymmetries may develop prenatally and/or during the earliest of periods of brain maturation. This differential specialization of the left and right hemisphere is not only critical for speech perception, language and visuospatial function (Toga and Thompson 2003), but is also important for emotional and other higher behavioral and cognitive traits, such as handedness, auditory perception, motor preferences and sensory acuity (Toga and Thompson 2003; Hugdahl and Davidson 2004).

Sexual dimorphism of the human brain has been well-established histologically, and more recently, through in vivo MRI studies. Many of these studies have investigated sex differences in adolescents and adults, showing the male brain to be approximately 8–10% greater in volume than the female brain (Giedd et al. 1996; Caviness et al. 1996; Goldstein et al. 2001); though this is not constant across gray and white matter regions. For example, after accounting for total brain volume, females have larger gray matter volume, whereas males typically have greater white matter volume (Caviness et al. 1996; Lenroot et al. 2007; Koolschijn and Crone 2013). Other findings of volume differentiation between males and females at birth are mixed, with few studies observing significant volumetric differences between males and females (Gilmore et al. 2007; Holland et al. 2014), and others observing no differences (Makki and Hagmann 2017).

Thus, important questions about infant brain maturation remain unaddressed. For instance, while volumetric measures of more general anatomic brain regions (i.e., frontal, parietal, temporal, occipital lobes) have been well studied in neonates and term infants (Hüppi et al. 1998a; Gilmore et al. 2007), developmental patterns of these measures within deep subcortical gray and white matter are less clear, in particular, throughout the first month of life. The study of such regional brain development is, however, essential to understanding the origins of typical neurodevelopment and potential disorders given the vulnerability of early brain development to many extrinsic and intrinsic influences (Andersen 2003). Moreover, given the limited and mixed findings of hemispheric lateralization and sexual dimorphism during this early life period, further study of these relationships is important to know whether such characteristics are present at the time of birth or whether they emerge throughout postnatal life. Such understanding in normative development is necessary prior to examining whether these characteristics are altered by disease or can be modified by early life experiences.

Utilizing high resolution structural MRI and infant brain atlases, we quantify regional gray and white matter volumes in a cohort of 1 month infants. We assess structural differences in relation to gestational age and examine emerging regional asymmetries as well as differences between males and females. In addition, we investigate associations between these regional brain measures and traditional markers of development, such as head circumference and birth weight and length. The analyses presented here build upon the findings from recent pediatric neuroimaging studies and highlight new insights into the underlying relationships of the infant brain during first month of life.

Materials and methods

Subjects

Participants were recruited as part of an ongoing longitudinal study investigating the influence of early life experience on brain and behavioral development. We recruited and enrolled 149 women during the second trimester of pregnancy (< 28 weeks' gestation) using the following inclusion and exclusion criteria: between 18 and 40 years of age, expecting singleton births, no diagnosis of major psychiatric illnesses (i.e., schizophrenia, bipolar disorder, borderline personality disorder), no pre-existing neurological conditions or major head trauma, no major autoimmune disease or infections during pregnancy and uncomplicated childbirth. Mothers confirmed the criteria through interviews prior to enrollment and through medical history questionnaires that were obtained as part of the study. Infants (77 female/72 male) were brought in to the MRI facility for imaging at 1 month of age. The total sample had a mean age of 34.1 days ± 7.7 days (corrected to a 40-week gestational period). Males and females were well matched with no significant differences on gestational age at MRI scan ($p = 0.14$), gestation length ($p = 0.97$), head circumference at birth ($p = 0.18$), birth weight ($p = 0.86$), or birth length ($p = 0.91$). Additional demographic information of the sample is provided in Table 1. The local Institutional Review Board approved all study procedures, and parental consent was obtained from each participating family.

MRI data acquisition

Infants underwent MR imaging during natural, non-sedated sleep (Dean et al. 2014a). Scans were scheduled to correspond with the infant's sleep schedule and typically occurred after the infant was fed and swaddled. Once asleep, infants were placed in the darkened MRI scanner where we utilized several techniques designed to enhance imaging data collection from a sleeping infant. First, to support infant sleep and comfort, intra-scan motion was limited by utilizing an infant MedVac vacuum immobilization bag (CFI Medical Solutions, USA) and foam cushions were placed around the infant's head. We also used a noise-attenuating foam insert in the bore of the MRI scanner and infants wore ear plugs, MiniMuff® (Natus Medical Incorporated) neonatal noise attenuating ear covers, and electrodynamic headphones (MR Confon, Germany) to limit the acoustic noise of the scan. We designed acoustically optimized imaging protocols that limited the peak gradient slew-rates of the MRI pulse sequence to help the infant remain asleep. Infants were monitored throughout the MRI scan by a research staff member, and mothers remained in the scanner room throughout the scan if they chose to do so.

Imaging data were acquired on a 3 T General Electric MR750 Discovery scanner using a 32 channel receive-only head RF array coil (Nova Medical, Wakefield, MA). Structural T_1- and T_2-weighted images were obtained using GE's 3D BRAVO (BRAin VOlume) and CUBE imaging pulse sequences, respectively. Images were sagittally acquired with a 1.0 mm^3 isotropic spatial resolution. To reduce the sound produced during the scan, the gradient slew rates were reduced by approximately 67% of their nominal value.

Table 1 Participant demographic characteristics

Sample characteristics	Combined	Males	Females	p value
N	149	72	77	
Mean ± standard deviation infant age (days)	34.1 ± 7.7	33.1 ± 7.2	35.0 ± 8.0	0.14
Mean ± standard deviation gestation (weeks)	39.6 ± 1.4	39.6 ± 1.3	39.6 ± 1.4	0.78
Mean ± standard deviation birth weight (kg)	3.49 ± 0.5	3.48 ± 0.5	3.49 ± 0.5	0.83
Mean ± standard deviation birth length (cm)	51.4 ± 2.6	51.4 ± 2.6	51.4 ± 2.6	0.98
Mean ± standard deviation head circumference (cm)	34.8 ± 1.5	35.0 ± 1.5	34.6 ± 1.5	0.18
APGAR score				
1 min (mean ± standard deviation)	8.0 ± 1.8	8.0 ± 1.8	8.0 ± 1.8	0.92
5 min (mean ± standard deviation)	8.8 ± 0.6	8.8 ± 0.7	8.9 ± 0.6	0.57
Mean maternal age (years)	33.4 ± 3.8	33.5 ± 3.8	33.2 ± 3.8	0.62
Maternal racial background				
African American/Black	3	0	3	
Asian	11	6	5	
Caucasian/White	130	66	64	
Native Hawaiian or Other Pacific Islander	1	0	1	
Native American Indian/Native Alaskan	2	0	2	
Not Reported	2	0	2	

Additional BRAVO imaging parameters included: repetition time (TR): 8.7 ms; echo time (TE): 3.4 ms; inversion time (TI): 450 ms; and flip angle: 12°; field of view (FOV): 25.6 cm × 25.6 cm × 17.0 cm; and an acquisition time of 8 min 10 s. CUBE imaging parameters were: TR: 2500 ms; FOV: 25.6 cm × 25.6 cm × 16.0 cm; echo train length: 65; and an acquisition time of 5 min and 36 s.

Additional images, including resting-state functional MRI, and multi-shell diffusion tensor imaging (DTI), were acquired as part of the research imaging protocol (total protocol acquisition: 49 min and 19 s). Analyses examining the multi-shell DTI data have been presented elsewhere (Dean et al. 2017).

Construction of 1-month T_1- and T_2-weighted brain templates

We created population-specific T_1- and T_2-weighted templates from a subset of 75 infants from which T_1- and T_2-weighted images were acquired and determined to be artifact free after visual inspection. These templates were created using symmetric diffeomorphic normalization and cross-correlation similarity measure (Avants et al. 2011a) as implemented in the distributed buildtemplateparallel.sh script as part of the Advanced Normalization Tools (ANTs) software package (http://stnava.github.io/ANTs/).

Two publicly available neonatal brain atlases, one including definitions of anatomical brain regions (Shi et al. 2011) and the other containing definitions of neonatal white matter tracts (Oishi et al. 2011), were used to define regions of interest (ROIs). These atlases were nonlinearly registered to the population-specific study template space using symmetric diffeomorphic normalization as implemented in ANTs and a mutual information criterion. Registrations were visually assessed to ensure alignment between the publicly available templates and the population-specific study template. Using nearest-neighbor interpolation, the anatomical and white matter priors were warped into the space of the population-specific study template.

Image preprocessing, normalization, and volume measurement

All T_1- and T_2-weighted images were manually assessed for motion and other image artifacts by a trained researcher (DD). If determined usable, images were skull-stripped using automated methods (Avants et al. 2011a). Resulting brain masks were assessed to ensure skull was completely removed and manually edited if necessary. Next, T_1- and T_2-weighted images were aligned to the population-specific template space. For infants with both T_1- and T_2-weighted images, a multivariate image registration approach with ANTs was utilized (Avants et al. 2011b). In this case, both T_1- and T_2-weighted images are used in the registration to the population-specific study template space, producing a single transformation that warps the T_1- and T_2-weighted images to the study template. Infants with only a usable T_1- or T_2-weighted image were registered to the appropriate corresponding population-specific study template with ANTs and symmetric diffeomorphic normalization.

Following normalization to the study template, volumes of subcortical gray matter and white matter regions were calculated. For each subject, the inverse warp transformation was applied to the anatomical and white matter priors, thus, transforming the priors into the native MRI space of each individual. Volumes of each ROI were then calculated. Subcortical gray matter regions of the amygdala, caudate, insula, cingulate gyrus (anterior, mid, and posterior sections), hippocampus, parahippocampal gyrus, pallidum, putamen, and thalamus were calculated; while white matter regions included the corpus callosum, internal capsules (anterior, posterior and retrolenticular limbs), sagittal stratum, and the superior longitudinal fasciculus.

To ensure that left and right regional brain volumes were not biased by potential left/right differences from the neonatal brain atlases, the left–right orientation of the subject's T_1- and/or T_2-weighted images was flipped and these flipped images were re-registered to the study template space, as previously described. Volumes of left and right homologous pairs for each subcortical region were then calculated by averaging the volumes of the non-flipped and flipped images.

Gross measures of brain structure, including total brain volume as well as total gray and white matter volume, were calculated from the corresponding masks estimated from the study-specific T_1- and T_2-weighted templates using FMRIB's Automated Segmentation Tool (FAST; Zhang et al. 2001). The inverse warp transformation was applied to these masks and the volumes were subsequently calculated for each subject.

Statistical analyses

Assessment of alignments to infant template

In addition to visual inspection of the registration of the atlas priors to the infant MRI data, we quantified the degree of overlap between the individual MRI data and neonatal atlases to verify the nonlinear registration of the infant MRI data to the neonatal atlases provided adequate alignments of the atlas priors. First, each subject's individual atlas priors were warped to the infant template space, using the inverse transformation calculated in the registration process. Then, for each subject, we compared the similarity of the original atlas priors to that of the infant's template aligned priors by computing percent volume difference, the Jaccard similarity coefficient, and Dice coefficient. Larger Jaccard similarity

and Dice coefficients and smaller percent volume differences indicate increased overlap between the original and infant aligned atlas priors.

Comparison of T_1- and T_2-weighted volume measurements

Increased water content and low levels of myelin in the neonatal brain results in T_2-weighted images having improved tissue contrast than T_1-weighted images at this early age (Paus et al. 2001; Dubois et al. 2014). Thus, T_2-weighted images are typically used for volume estimation in infants. However, volume estimation using T_1-weighted images is possible and could provide measurements for subjects that do not have a usable T_2-weighted image (e.g., motion corrupted or not acquired due to waking in the scanner). Moreover, incorporating both T_1- and T_2-weighted images into a multivariate normalization framework may improve the alignment to the study template and thus provide more accurate volume estimates (Avants et al. 2011b). Thus, to examine whether volume estimates from the developed processing pipeline are dependent on the choice of image modality, we first compared volume estimates calculated separately from the T_1- and T_2-weighted images, as well as calculated from T_1- and T_2-weighted images that underwent multivariate normalization. We restricted this analysis to the subset of subjects that had successful T_1- and T_2-weighted scans acquired. Pearson correlations and paired *t* tests were used to compare the volume estimates from each case.

Regional asymmetry

Volumetric asymmetry between left and right homologous subcortical regions was compared by computing an asymmetry index (AI) for each subject using the following formula: $AI = 100 \times (Left–Right)/(Left+Right)$. This index can range from -100 to 100, where positive values correspond to leftward asymmetry and negative values correspond to rightward asymmetry. A single sample *t* test was used to test whether asymmetry indices differed from zero. We used a Bonferroni correction to account for multiple comparisons and significance was defined as $\alpha < 0.003$ ($p < 0.05$, Bonferroni corrected for the 17 left–right homologous pairs examined).

Sex differences

One-way analyses of variance (ANOVAs) compared brain regions between males and females, including gestational-corrected age and total brain volume as covariates. Furthermore, in regions that were observed to have a left–right difference, we examined whether male–female difference was associated with the brain asymmetry by comparing AIs between males and females, accounting for gestational age and total brain volume. For all analyses, significance was defined as $p < 0.05$, Bonferroni corrected for multiple comparisons.

Within age relations

Although we attempted to test infants at a constant age (1 month), some variation in age of testing occurred. Thus, we included analyses of within age variability in brain structure to examine associations between gestational corrected age and regional brain volumes. Linear models including sex and an age-by-sex interaction to examine potential differences between males and females were fit to volumetric data using ordinary least squares minimization.

Relations with markers of newborn growth

Newborn growth measures, including head circumference, birth weight and birth length, were acquired from participant medical records. Partial correlations assessed relations between volumetric brain measures and these newborn growth measures, controlling for total brain volume and gestational age. Significance was defined as $p < 0.05$ (Bonferroni corrected).

All statistical analyses were performed using R version 3.3.3 (R Development Team 2014).
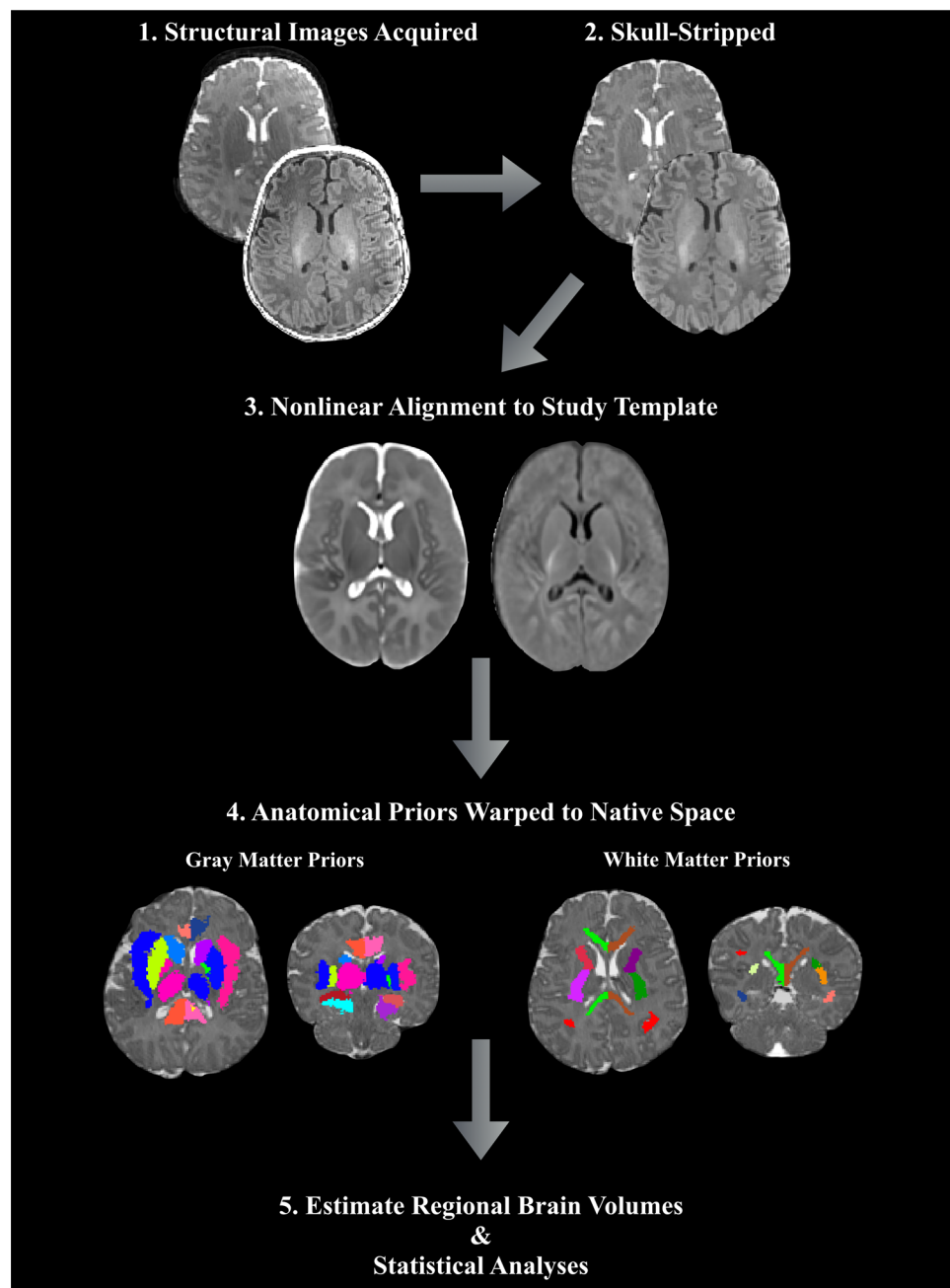
Results

From the full cohort of 149, a usable T_1- or T_2-weighted image was successfully acquired from 143 (73 female) of the 1-month-old infants. Of these, 125 had usable T_1- and T_2-weighted images, 13 had a usable T_2-weighted image, and 5 had a usable T_1-weighted image. Infants without usable imaging data ($N=6$) did not fall asleep, woke up during the scan acquisition, or acquired data were corrupted by motion artifacts. These six subjects were thus excluded from subsequent analyses. No significant demographic differences were observed between the full cohort of enrolled infants and the infants in which usable MRI data were acquired (Fig. 1).

Assessment of alignments to infant template

Axial and coronal views of the study specific structural T_1- and T_2-weighted templates are shown in Fig. 2. Coregistered atlas priors used in subsequent analyses from the structural (Shi et al. 2011) and white matter (Oishi et al. 2011) neonate brain atlases are also displayed in Fig. 2. All successfully acquired individual images were registered to these templates using symmetric diffeomorphic

Fig. 1 Overview of the image processing and volume calculation pipeline. Upon acquisition and inspection of T_1- and T_2-weighted images, non-parenchyma tissue is removed and images are aligned to the study-specific template. Subcortical gray matter and white matter atlas priors are then inverse warped to the infant native space and regional volumes are computed

registration with ANTs (Avants et al. 2011a). Representative individual T_1- and T_2-weighted images aligned in the template space are displayed in Fig. 3. Superimposition of the atlas priors to the infant data was quantitatively assessed by computing percent volume differences, Jaccard similarity and Dice coefficient (Supplementary Table 1). Across all brain regions, the average percent volume difference, Jaccard similarity, and Dice coefficient between the original atlas priors and the infant atlas priors was 0.72, 88.31, and 93.75%, respectively. Total gray matter volume was observed to be the most discrepant brain region, with an average percent volume difference, Jaccard similarity, and Dice coefficient of 2.04, 90.06, and 81.94%. Right middle cingulate gyrus had the smallest percent volume difference (0.24%), while total brain volume had the largest Jaccard similarity (98.52%) and Dice coefficient (99.25%). Overall, these results qualitatively and quantitatively demonstrate the ability of the symmetric diffeomorphic registration to provide accurate alignment between the 1-month brain to the study-specific template space.
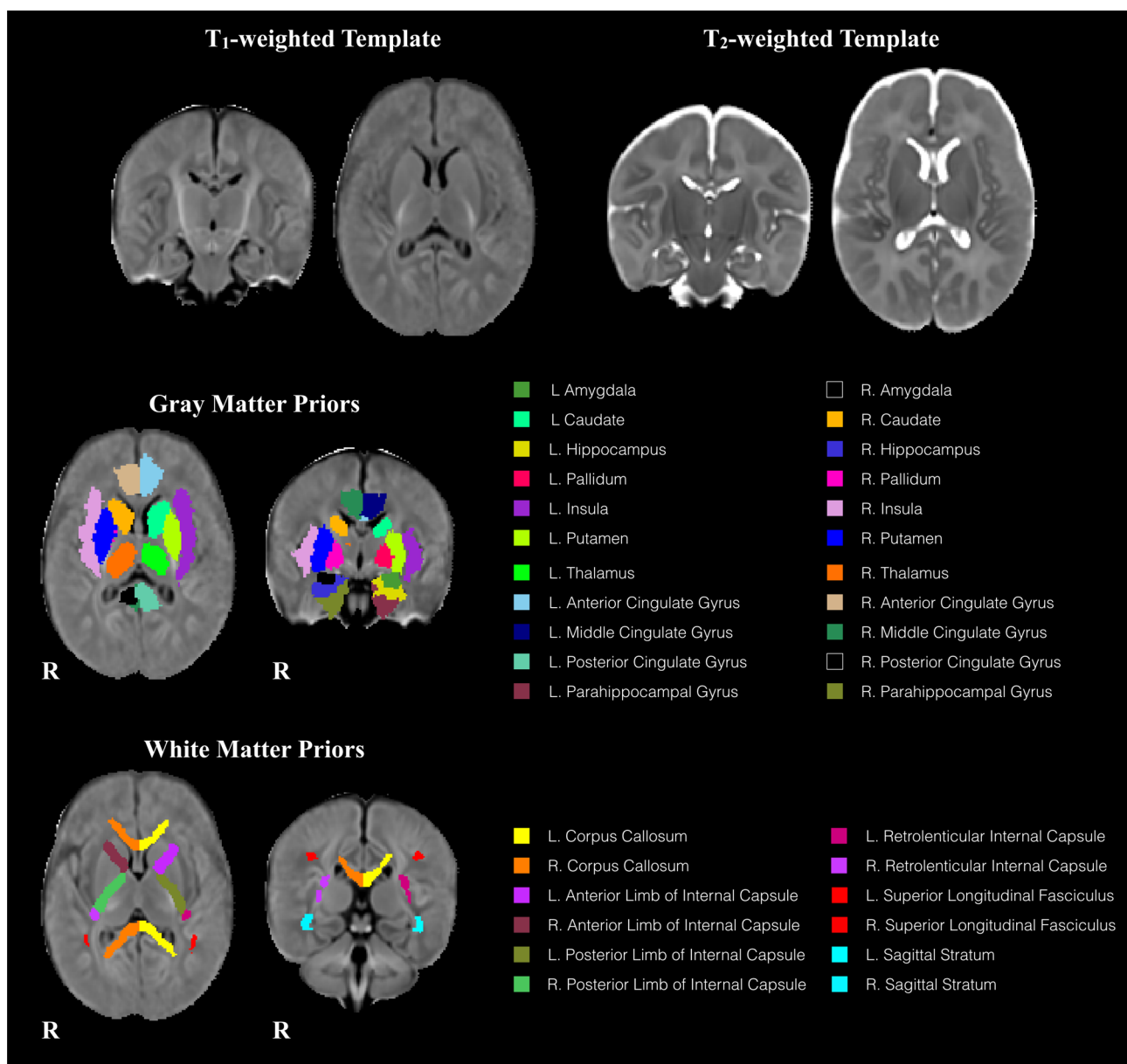
Fig. 2 Top row: representative axial and coronal views of the study-specific T$_1$-weighted and T$_2$-weighted templates generated from 1-month-old infant brain data. Middle row: subcortical gray matter and bottom row: white matter regions used for volumetric measurement. Regions are overlaid on the T$_1$-weighted template and separated by color

Comparison of T$_1$- and T$_2$-weighted volume measurements

A scatter plot illustrating correlations between the volumes measured from T$_1$-weighted and T$_2$-weighted images is shown in Fig. 4 (see Supplementary Figs. 1 and 2 for comparison with multivariate T$_1$-weighted and T$_2$-weighted normalization strategy). Volumes measured from T$_1$-weighted images were significantly correlated with volumes measured from T$_2$-weighted images (mean $r = 0.7095 \pm 0.10$; $p < 0.00001$); while volumes measured from the multivariate T$_1$- and T$_2$-weighted normalization strategy were also significantly related to the volumes measured from the T$_2$-weighted images (mean $r = 0.7867 \pm 0.10$; $p < 0.00001$) and T$_1$-weighted images (mean $r = 0.7462 \pm 010$; $p < 0.00001$). Furthermore, no significant paired differences were observed between each of the volume estimation techniques (Supplementary Table 2). Given the high degree of correlation and no significant differences between these volume measurements, we found it appropriate to use data from all subjects with usable T$_1$- or T$_2$-weighted images ($N = 143$) in subsequent analyses.
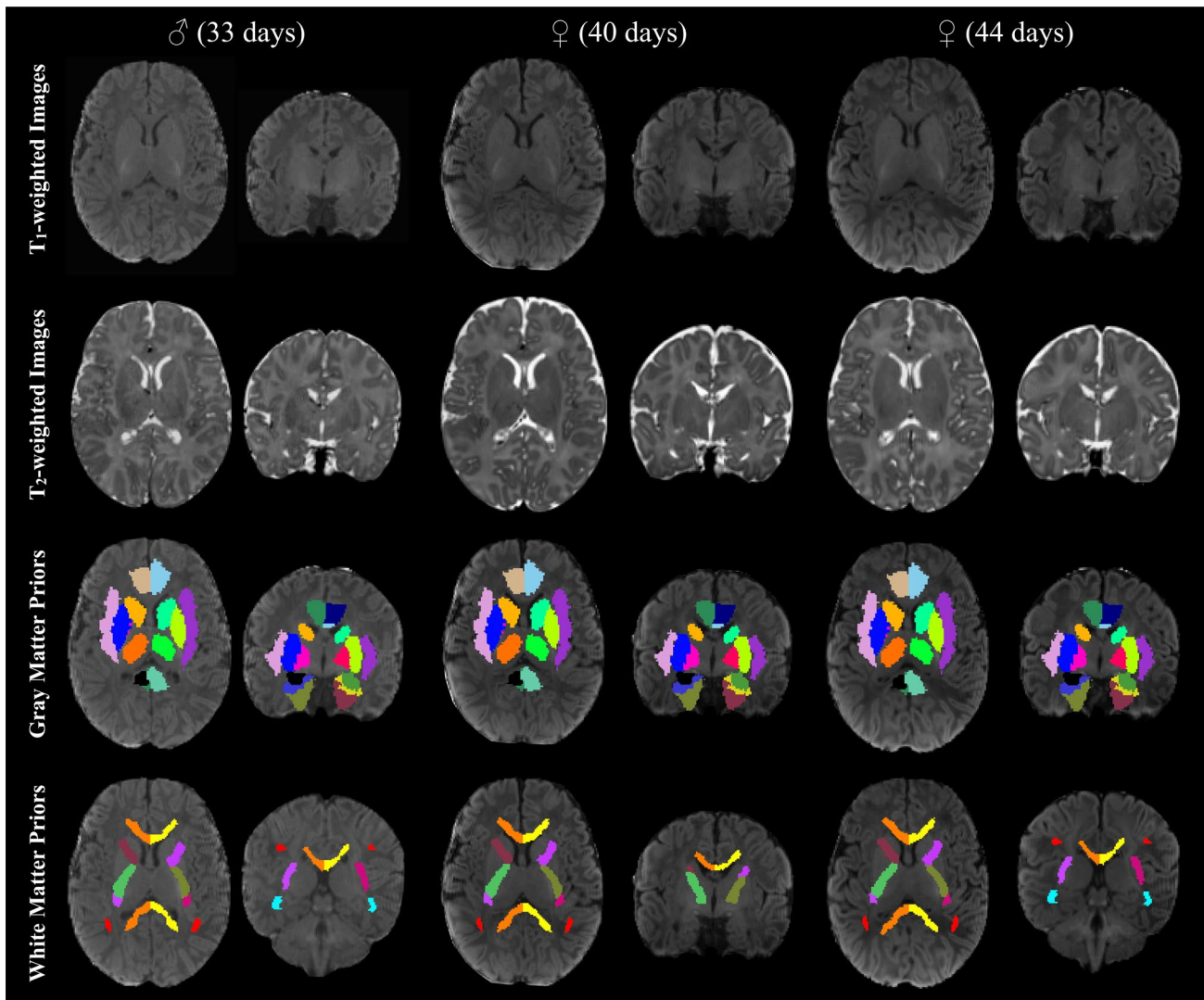
Fig. 3 Individual T_1- and T_2-weighted images aligned to the study specific template space, with subcortical gray and white matter priors overlaid on the individual's T_1-weighted image. Subcortical gray matter and white matter regions are color-coded as in Fig. 2. These representative images demonstrate the ability of the symmetric diffeomorphic registration to successfully map T_1- and T_2-weighted images to the study-specific template space, while quantitative assessment of overlap shows evidence for good agreement between atlas and individual priors (Supplementary Table 1)

Regional asymmetry, sex differences, and age relations

Regional brain volumes (13 of 17) exhibited significant left/right asymmetry in all examined regions but the posterior cingulate gyrus, corpus callosum, anterior limb of the internal capsule, and sagittal stratum. Asymmetry results are presented in Table 2, and asymmetry indices plotted as a function of gestation-corrected age for a representative subset of examined brain regions are in Supplementary Fig. 3. We observed a significant ($p < 0.05$, corrected) rightward asymmetry in many of the gray matter brain regions, including the amygdala, thalamus, putamen, hippocampus, and caudate.

Left hemisphere white matter volumes, including the posterior and retrolenticular limbs of the internal capsule and the superior longitudinal fasciculus were found to be larger than the left hemisphere white matter volumes. Age and sex did not relate to asymmetry.

Significant volumetric differences between males and females were detected across all the examined brain regions (see Table 3). In general, volumetric measures in males were larger than females; however, these differences correlated with overall differences in total brain volume. Upon correcting for total brain volume differences, sexual dimorphism in the 1-month infant brain remained. Males had a significantly larger total brain and white matter volume; while also having
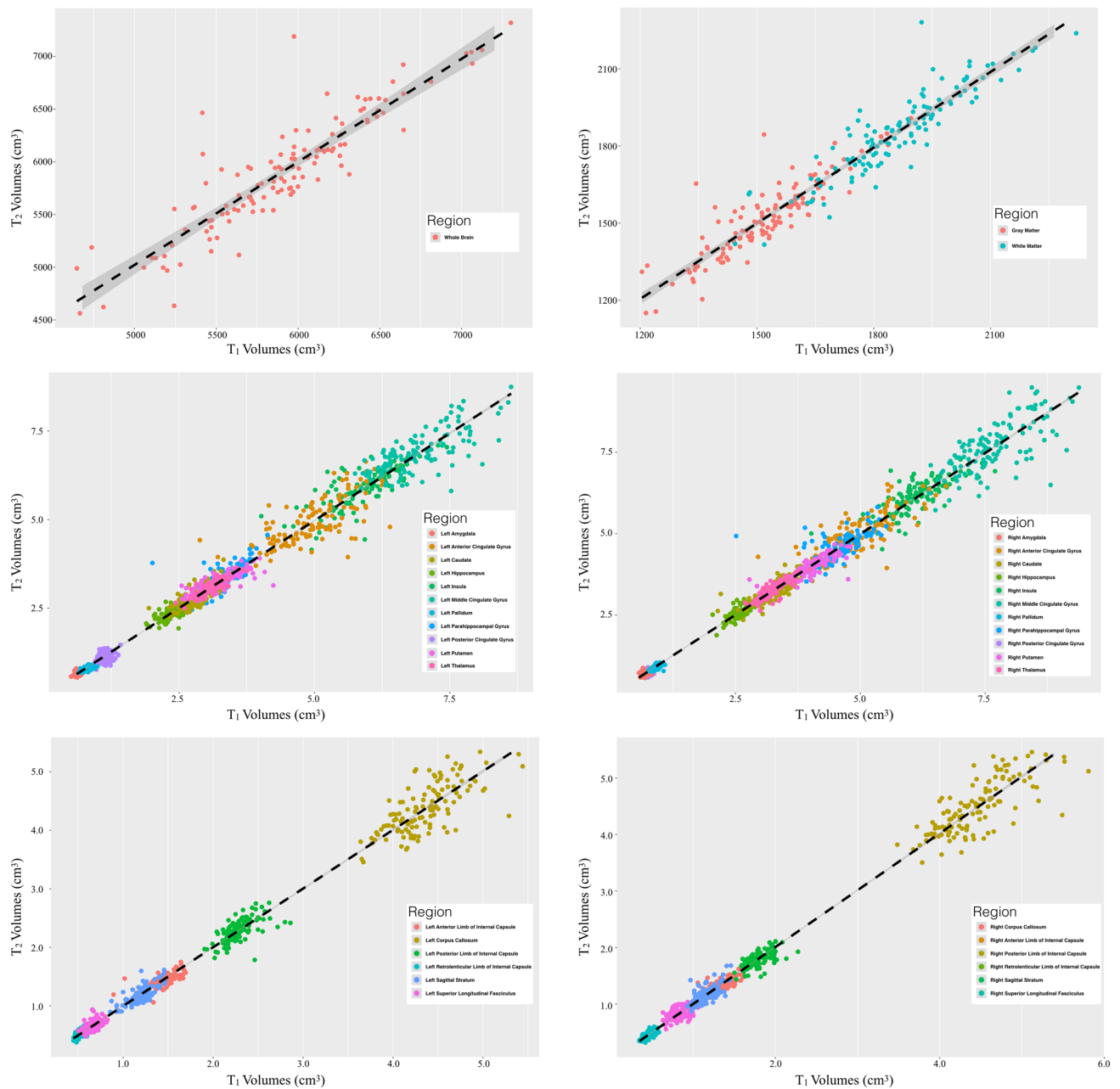
Fig. 4 Correlations between infant brain volumes measured using T_1-weighted and T_2-weighted images (for comparison with multivariate normalization, see Supplementary Figs. 1 and 2). Estimated volumes were found to all be highly correlated and thus we used measurements from both T_1- and T_2-weighted images

larger amygdala, insula, hippocampus, thalamus, pallidum, and putamen volumes. Females displayed larger volumes of the anterior and middle cingulate gyrus, caudate and parahippocampal gyrus, as well as white matter regions of the corpus callosum and right hemisphere posterior and retrolenticular limbs of the internal capsule. Females had approximately 8.7% larger corpus callosum volume, after correcting for total brain volume. The magnitude of these structural differences was similar between males and females, with males having $8.23 \pm 1.10\%$ greater volume in male > female regions, while females had $8.09 \pm 1.55\%$ greater volume in female > male brain regions. Analyses designed to investigate whether sex differences varied as a factor of gestational age in days revealed no significant findings.

Though infants were all approximately 1 month of age, there was variability in gestational corrected age which related to and regional brain volumes (Table 4). Total brain volume (Fig. 5), gray matter volume, and white matter

Table 2 Comparison of left and right hemisphere brain regions

	Left hemisphere	Right hemisphere	T	p value	Percent difference (%)	Direction
Gray matter regions						
Amygdala	0.7009 ± 0.07	0.7423 ± 0.08	11.79	**< 0.001**	− 2.84	Rightward
Caudate	2.9249 ± 0.32	2.9702 ± 0.33	4.63	**< 0.001**	− 0.76	Rightward
Hippocampus	2.4940 ± 0.24	2.603 ± 0.24	10.37	**< 0.001**	− 2.15	Rightward
Putamen	3.5264 ± 0.34	3.7059 ± 0.36	11.94	**< 0.001**	− 2.47	Rightward
Pallidum	0.7934 ± 0.07	0.8195 ± 0.08	6.89	**< 0.001**	− 1.60	Rightward
Insula	5.7975 ± 0.59	6.0112 ± 0.63	7.74	**< 0.001**	− 1.79	Rightward
Thalamus	3.0587 ± 0.26	3.0944 ± 0.27	3.77	**< 0.001**	− 0.56	Rightward
Anterior cingulate gyrus	4.9361 ± 0.65	5.0873 ± 0.68	8.42	**< 0.001**	− 1.50	Rightward
Middle cingulate gyrus	7.1151 ± 0.77	7.2217 ± 0.82	5.81	**< 0.001**	− 0.71	Rightward
Posterior cingulate gyrus	0.9130 ± 0.11	0.9195 ± 0.1	1.28	0.20	− 0.43	–
Parahippocampal gyrus	3.9052 ± 0.40	4.1013 ± 0.41	12.45	**< 0.001**	− 2.45	Rightward
White matter regions						
Corpus callosum	4.4142 ± 0.47	4.3896 ± 0.49	1.80	0.074	0.30	–
Anterior limb of internal capsule	1.3453 ± 0.14	1.3347 ± 0.14	2.01	0.046	0.38	–
Posterior limb of internal capsule	1.9914 ± 0.20	1.9066 ± 0.18	9.15	**< 0.001**	2.15	Leftward
Retrolenticular limb of internal capsule	0.4784 ± 0.05	0.4484 ± 0.05	8.23	**< 0.001**	3.27	Leftward
Superior longitudinal fasciculus	0.7576 ± 0.08	0.7212 ± 0.09	6.98	**< 0.001**	2.52	Leftward
Sagittal stratum	1.1619 ± 0.12	1.1515 ± 0.13	1.64	0.104	0.49	–

Mean ± standard deviation of regional brain volumes are reported in cm^3. Significance was defined as $p < 0.05$ (Bonferroni corrected for multiple comparisons) corresponding to $p < 0.003$. p values meeting the significance criteria are bolded

volume were all related to variability within infant gestational age, indicating that the brain is rapidly developing at 1 month. Several subcortical gray matter brain regions, including the amygdala, hippocampus, caudate, insula, and parahippocampal gyrus, also varied within age (Supplemental Fig. 4). The right and left hemisphere volumes of the corpus callosum and posterior limbs of the internal capsule, as well as the left hemisphere retrolenticular limb of the internal capsule and sagittal stratum were also observed to significantly vary with age, though the remaining white matter volumes were trending ($p < 0.05$, uncorrected). Model slope estimates (Table 4) differed between brain regions, suggesting that specific brain regions develop at different rates. Males and females exhibited similar age-related differences across bilateral brain regions. However, for several brain regions (right amygdala, left caudate, right insula, thalamus, corpus callosum, and posterior and retrolenticular limbs of the internal capsule), a trend level ($p < 0.05$, uncorrected) sex difference in gestational age differences was observed.

Relations with markers of newborn growth

Medical records that included head circumference, birth weight, and birth length were available for 127 of the 143 infants. Associations of these measures with regional brain

volumes were examined from this subset and the results are provided in Table 5. Total brain volume was significantly associated with head circumference at birth ($p < 0.001$, corrected). After correcting for gestational age and total brain volume, the left putamen, insula and right posterior limb of the internal capsule were positively related to birth weight. No other brain region was significantly associated with these newborn growth measures.

Discussion

Using regional brain volumes measured from high resolution structural T_1 and T_2-weighted MRI, we investigated patterns of brain maturation in the 1-month infant. From a cohort of 143 infants, results indicated that both the overall brain macrostructure and underlying subcortical brain regions undergo sex- and age-related changes within the first month of life. Our results provide further evidence that structural asymmetries and sexual dimorphism already exists at 1 month of life, suggesting that these characteristics emerge throughout the prenatal period and first weeks of life. We additionally examined relations between infant volumetric brain measures and newborn growth metrics of head circumference, birth weight, and birth length, and found only total brain volume and the volumes of the

Table 3 Comparison of volumetric brain measures between males and females

	Male	Female	F	p value	Percent difference (%)	Direction
Total brain volume	611.48 ± 47.5	562.7 ± 50.6	41.86	**< 0.001**	8.32	Male
Gray matter	158.68 ± 12.9	146.22 ± 13.4	4646.67	**< 0.001**	8.18	Female
White matter	194.91 ± 15	179.21 ± 15.1	620.32	**< 0.001**	8.40	Male
Gray matter regions						
Left amygdala	0.73 ± 0.1	0.67 ± 0.1	89.8	**< 0.001**	9.11	Male
Right amygdala	0.78 ± 0.1	0.71 ± 0.1	109.9	**< 0.001**	10.04	Male
Left caudate	3.05 ± 0.3	2.81 ± 0.3	64.9	**< 0.001**	8.23	Female
Right caudate	3.09 ± 0.3	2.85 ± 0.3	54.6	**< 0.001**	8.02	Female
Left hippocampus	2.6 ± 0.2	2.4 ± 0.2	92.2	**< 0.001**	8.09	Male
Right hippocampus	2.71 ± 0.2	2.5 ± 0.2	92.9	**< 0.001**	7.86	Male
Left putamen	3.66 ± 0.3	3.4 ± 0.3	58.7	**< 0.001**	7.57	Male
Right putamen	3.87 ± 0.3	3.55 ± 0.3	76.0	**< 0.001**	8.46	Male
Left pallidum	0.82 ± 0.1	0.77 ± 0.1	40.2	**< 0.001**	6.81	Male
Right pallidum	0.85 ± 0.1	0.79 ± 0.1	48.9	**< 0.001**	7.65	Male
Left insula	6.01 ± 0.6	5.59 ± 0.5	55.8	**< 0.001**	7.15	Male
Right insula	6.26 ± 0.6	5.77 ± 0.5	75.5	**< 0.001**	8.11	Male
Left thalamus	3.17 ± 0.2	2.96 ± 0.2	84.9	**< 0.001**	6.91	Male
Right thalamus	3.21 ± 0.3	2.99 ± 0.2	56.5	**< 0.001**	7.04	Male
Left anterior cingulate gyrus	5.21 ± 0.7	4.68 ± 0.5	100.9	**< 0.001**	10.79	Female
Right anterior cingulate gyrus	5.36 ± 0.7	4.82 ± 0.6	99.1	**< 0.001**	10.64	Female
Left middle cingulate gyrus	7.42 ± 0.7	6.82 ± 0.7	78.0	**< 0.001**	8.51	Female
Right middle cingulate gyrus	7.53 ± 0.8	6.93 ± 0.7	69.0	**< 0.001**	8.25	Female
Left posterior cingulate gyrus	0.96 ± 0.1	0.87 ± 0.1	36.7	**< 0.001**	9.14	Male
Right posterior cingulate gyrus	0.96 ± 0.1	0.88 ± 0.1	74.3	**< 0.001**	9.09	Male
Left parahippocampal gyrus	4.04 ± 0.4	3.77 ± 0.4	54.5	**< 0.001**	6.97	Female
Right parahippocampal gyrus	4.24 ± 0.4	3.97 ± 0.4	46.6	**< 0.001**	6.66	Female
White matter regions						
Left corpus callosum	4.61 ± 0.4	4.23 ± 0.4	87.98	**< 0.001**	8.54	Female
Right corpus callosum	4.59 ± 0.5	4.2 ± 0.4	74.95	**< 0.001**	8.80	Female
Left anterior limb of internal capsule	1.4 ± 0.1	1.29 ± 0.1	50.51	**< 0.001**	8.29	Male
Right anterior limb of internal capsule	1.39 ± 0.1	1.29 ± 0.1	42.05	**< 0.001**	7.45	Male
Left posterior limb of internal capsule	2.06 ± 0.2	1.93 ± 0.2	32.2	**< 0.001**	6.44	Male
Right posterior limb of internal capsule	1.97 ± 0.2	1.85 ± 0.2	32.5	**< 0.001**	6.13	Female
Left retrolenticular limb of internal capsule	0.49 ± 0.1	0.46 ± 0	23.8	**< 0.001**	6.60	Male
Right retrolenticular limb of internal capsule	0.46 ± 0.1	0.44 ± 0	13.4	**< 0.001**	5.43	Female
Left superior longitudinal fasciculus	0.79 ± 0.1	0.72 ± 0.1	57.30	**< 0.001**	9.34	Male
Right superior longitudinal fasciculus	0.76 ± 0.1	0.68 ± 0.1	48.73	**< 0.001**	10.26	Male
Left sagittal stratum	1.22 ± 0.1	1.11 ± 0.1	96.68	**< 0.001**	9.44	Male
Right sagittal stratum	1.21 ± 0.1	1.1 ± 0.1	81.13	**< 0.001**	9.85	Male

Mean ± standard deviation of regional brain volumes is reported in mm^3. Significance was defined as $p < 0.05$ (Bonferroni corrected for multiple comparisons) corresponding to $p < 0.00135$. p values meeting the significance criteria are bolded. Regions without left/right pairs did exhibit regional asymmetry and were combined to assess sex differences. n.s. denotes non-significant sex difference

putamen, insula and posterior limb of the internal capsule to be associated with these measures. Results from the present study complement as well as build upon findings of a growing corpus of studies that seek to better understand infant brain development.

Regional brain asymmetry

We detected widespread regional asymmetries among subcortical brain regions. White matter volumes were lateralized to the left-hemisphere, with the posterior and retrolenticular

Table 4 Relationships of volumetric brain measures and gestation corrected age

	Age			Age × sex		
	Estimate	T	p value	Estimate	T	p value
Total brain volume	3448.53	4.34	**< 0.001**	− 1342.73	− 1.31	0.190
Gray matter	936.23	4.44	**< 0.001**	− 348.05	− 1.28	0.200
White matter	1064.65	4.31	**< 0.001**	− 561.85	− 1.76	0.080
Gray matter regions						
Left amygdala	3.73	3.43	**0.001**	− 1.91	− 1.36	0.18
Right amygdala	4.88	4.18	**< 0.001**	− 2.93	− 1.95	0.050
Left caudate	20.24	4.03	**< 0.001**	− 13.72	− 2.12	0.040
Right caudate	18.16	3.49	**0.001**	− 11.08	− 1.65	0.100
Left hippocampus	13.58	3.75	**< 0.001**	− 5.96	− 1.27	0.200
Right hippocampus	13.45	3.70	**< 0.001**	− 4.28	− 0.91	0.360
Left putamen	18.21	3.50	**0.001**	− 10.12	− 1.51	0.130
Right putamen	23.73	4.42	**< 0.001**	− 13.00	− 1.88	0.060
Left pallidum	2.84	2.32	0.022	− 2.01	− 1.28	0.200
Right pallidum	3.46	2.77	0.006	− 1.66	− 1.03	0.310
Left insula	39.25	4.39	**< 0.001**	− 18.65	− 1.62	0.110
Right insula	50.88	5.65	**< 0.001**	− 27.75	− 2.39	0.020
Left thalamus	16.03	4.14	**< 0.001**	− 9.76	− 1.95	0.05
Right thalamus	19.65	4.78	**< 0.001**	− 13.59	− 2.56	0.01
Left anterior cingulate gyrus	32.38	3.17	0.002	− 19.55	− 1.48	0.140
Right anterior cingulate gyrus	37.90	3.58	**< 0.001**	− 25.15	− 1.84	0.070
Left middle cingulate gyrus	40.69	3.37	**0.001**	− 29.75	− 1.91	0.060
Right middle cingulate gyrus	43.04	3.31	**0.001**	− 31.72	− 1.89	0.060
Left posterior cingulate gyrus	0.57	0.32	0.751	− 0.47	− 0.20	0.84
Right posterior cingulate gyrus	3.33	2.18	0.031	− 2.22	− 1.13	0.260
Left parahippocampal gyrus	18.42	2.92	**0.004**	− 5.40	− 0.66	0.510
Right parahippocampal gyrus	23.24	3.53	**0.001**	− 11.89	− 1.40	0.160
White matter regions						
Left corpus callosum	24.88	3.37	**0.001**	− 22.12	− 2.32	0.02
Right corpus callosum	25.82	3.36	**0.001**	− 24.69	− 2.49	0.010
Left anterior limb of internal capsule	5.66	2.52	0.013	− 1.50	− 0.52	0.600
Right anterior limb of internal capsule	5.40	2.45	0.015	− 2.00	− 0.70	0.48
Left posterior limb of internal capsule	15.58	5.02	**< 0.001**	− 10.34	− 2.58	0.01
Right posterior limb of internal capsule	13.16	4.54	**< 0.001**	− 9.55	− 2.55	0.010
Left retrolenticular limb of internal capsule	3.70	4.60	**< 0.001**	− 2.45	− 2.37	0.020
Right retrolenticular limb of internal capsule	2.80	3.20	0.002	− 2.27	− 2.01	0.050
Left superior longitudinal fasciculus	3.54	2.65	0.009	− 2.05	− 1.19	0.240
Right superior longitudinal fasciculus	2.95	2.08	0.040	− 1.37	− 0.75	0.460
Left sagittal stratum	7.22	3.99	**< 0.001**	− 2.50	− 1.07	0.290
Right sagittal stratum	5.34	2.67	0.009	− 1.11	− 0.43	0.670

Significance was defined as $p < 0.05$ (Bonferroni corrected for multiple comparisons) corresponding to $p < 0.00135$. p values meeting the significance criteria are bolded. n.s. denotes regions in which the sex-by-age interaction was not tested due to the interaction model not providing an adequate fit when compared to the nested age model

limbs of the internal capsule and superior longitudinal fasciculus, exhibiting significant regional asymmetries. Subcortical gray matter regions were found to be rightward asymmetric. For example, the amygdala, caudate, hippocampus, putamen, pallidum, insula, thalamus, anterior and middle cingulate gyrus, and parahippocampal gyrus volumes were larger in the right hemisphere, while the posterior cingulate gyrus was the only subcortical gray matter volume found not to exhibit asymmetry (Table 2). This pattern of results align with previous studies of older children and adults (Giedd
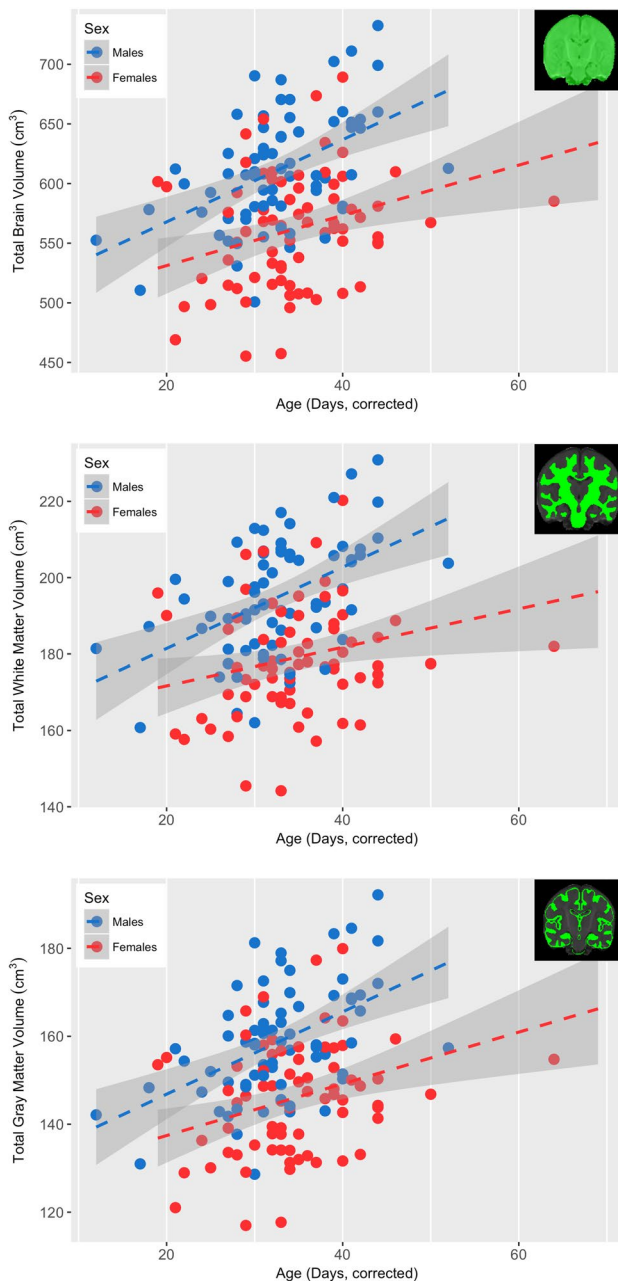
Fig. 5 Association between gestation corrected and total brain volume, white matter volume, and gray matter volume for males (blue) and females (red). Total brain volume was observed to significantly increase ($p < 0.05$, Bonferroni corrected) in both males and females, though this rate of increase did not differ between the two sexes

et al. 1996; Caviness et al. 1996; Holland et al. 2014), while also suggesting that such structural asymmetries begin to develop early in life (Dehaene-Lambertz et al. 2006). Regional asymmetries did not vary with gestational age, indicating relative stability throughout the first month of life. While this supports previous work examining structural brain asymmetry (Hill et al. 2010; O'Muircheartaigh et al. 2013), other work has reported asymmetry patterns to

change throughout development (Dehaene-Lambertz et al. 2006; Holland et al. 2014). However, studies observing such developmental asymmetry changes have typically examined brain changes across a larger age range than included in the current study (Holland et al. 2014). Thus, the age range of the current sample may limit our sensitivity to observe asymmetry changes. Nonetheless, as lateralization of the brain is important for functional specialization (Toga and Thompson 2003; Dubois et al. 2009), the emergence of these structural asymmetries is a fundamental characteristic of early brain development.

Differences between males and females

Males had larger total brain, gray, and white matter volumes than females. The magnitude of total brain volume differences was approximately 8.3%, similar to differences typically observed in adults (Lenroot and Giedd 2010) and other investigations of infant male/female brain differences (Gilmore et al. 2007; Knickmeyer et al. 2008; Holland et al. 2014). Similar to volumetric comparisons during infancy (Gilmore et al. 2007; Holland et al. 2014) and adolescence (Reiss et al. 1996; Wilke et al. 2007), after correcting for total brain volume, males had approximately 8.4% more white matter volume compared to females. These male/female differences, however, were smaller than those reported in adults (Allen et al. 2003), suggesting that the magnitude of these sex differences increases during development. Age-related changes did not differ between males and females in the limited age range that we examined. It is likely that over more extended age ranges, the ability to detect such developmental change could be improved. Indeed, developmental changes between males and females have been observed in other studies examining brain development across a more widespread age range (Lenroot and Giedd 2010; Giedd and Rapoport 2010).

Subcortical brain region volumes also differed between males and females. After correcting for total brain volume, females had larger volumes of the anterior and middle cingulate gyrus, parahippocampal gyrus, and caudate, as well as white matter regions of the corpus callosum, right hemisphere posterior and retrolenticular limbs of the internal capsule. In contrast, amygdala, insula, posterior cingulate gyrus, hippocampus, pallidum, thalamus, and putamen volumes were larger in males (Table 3). Female anterior cingulate gyrus volumes were ~ 10.7% larger than males. Our results suggesting males have larger amygdalae and hippocampi volumes differs from patterns observed later in life (Lenroot and Giedd 2010). Such sex differences, however, are likely to be influenced by sex steroid levels which can have a significant impact on cortical development (Lenroot and Giedd 2010). Thus, the sexual dimorphic relations observed during infancy may change over

Table 5 Comparison of regional brain volumes with newborn growth markers

	Head circumference			Birth weight			Birth length		
	r	T	p value	r	T	p value	r	T	p value
Total brain volume	0.486	6.196	**<0.001**	0.123	1.383	0.169	0.084	0.942	0.348
Gray matter	0.020	0.226	0.822	− 0.028	− 0.306	0.760	− 0.018	− 0.199	0.842
White matter	0.067	0.746	0.457	0.131	1.464	0.146	0.059	0.657	0.512
Gray matter regions									
Left amygdala	− 0.027	− 0.298	0.766	0.106	1.181	0.240	0.000	0.000	1.000
Right amygdala	− 0.127	− 1.419	0.158	0.003	0.032	0.974	0.023	0.253	0.801
Left caudate	0.138	1.549	0.124	0.205	2.320	0.022	0.091	1.009	0.315
Right caudate	0.152	1.701	0.091	0.223	2.532	0.013	0.098	1.091	0.278
Left hippocampus	0.017	0.187	0.852	0.058	0.640	0.523	− 0.033	− 0.363	0.717
Right hippocampus	− 0.061	− 0.682	0.497	− 0.034	− 0.382	0.703	− 0.053	− 0.584	0.560
Left putamen	0.117	1.302	0.195	0.315	3.687	**<0.001**	0.090	1.002	0.318
Right putamen	0.057	0.630	0.530	0.074	0.827	0.410	0.065	0.722	0.472
Left pallidum	0.016	0.176	0.861	0.206	2.340	0.021	0.031	0.341	0.734
Right pallidum	− 0.080	− 0.886	0.377	− 0.047	− 0.521	0.603	0.031	0.347	0.729
Left insula	0.059	0.655	0.513	0.361	4.289	**<0.001**	0.150	1.678	0.096
Right insula	0.079	0.882	0.380	0.148	1.665	0.098	0.190	2.147	0.034
Left thalamus	0.034	0.377	0.707	0.047	0.521	0.603	− 0.022	− 0.243	0.808
Right thalamus	− 0.051	− 0.567	0.572	− 0.055	− 0.612	0.542	0.015	0.166	0.869
Left anterior cingulate gyrus	− 0.038	− 0.421	0.674	− 0.030	− 0.328	0.743	− 0.092	− 1.030	0.305
Right anterior cingulate gyrus	− 0.147	− 1.648	0.102	− 0.069	− 0.772	0.442	− 0.152	− 1.703	0.091
Left middle cingulate gyrus	− 0.051	− 0.566	0.572	− 0.027	− 0.297	0.767	− 0.097	− 1.084	0.281
Right middle cingulate gyrus	0.002	0.025	0.980	0.005	0.059	0.953	0.001	0.009	0.993
Left posterior cingulate gyrus	− 0.018	− 0.202	0.840	− 0.045	− 0.501	0.617	− 0.056	− 0.625	0.533
Right posterior cingulate gyrus	− 0.048	− 0.536	0.593	− 0.058	− 0.641	0.523	− 0.036	− 0.401	0.689
Left parahippocampal gyrus	− 0.138	− 1.545	0.125	− 0.016	− 0.177	0.860	− 0.082	− 0.915	0.362
Right parahippocampal gyrus	− 0.205	− 2.321	0.022	− 0.112	− 1.248	0.214	− 0.149	− 1.676	0.096
White matter regions									
Left corpus callosum	0.124	1.389	0.167	0.091	1.008	0.315	0.050	0.552	0.582
Right corpus callosum	0.131	1.467	0.145	0.088	0.980	0.329	0.016	0.172	0.864
Left anterior limb of internal capsule	0.022	0.244	0.808	0.125	1.397	0.165	0.053	0.589	0.557
Right anterior limb of internal capsule	0.030	0.331	0.741	0.218	2.483	0.014	0.122	1.367	0.174
Left posterior limb of internal capsule	0.087	0.970	0.334	0.079	0.882	0.380	0.082	0.913	0.363
Right posterior limb of internal capsule	0.173	1.946	0.054	0.331	3.886	**<0.001**	0.134	1.502	0.136
Left retrolenticular limb of internal capsule	0.060	0.663	0.509	0.074	0.828	0.409	0.095	1.058	0.292
Right retrolenticular limb of internal capsule	0.094	1.047	0.297	0.184	2.075	0.040	0.115	1.289	0.200
Left superior longitudinal fasciculus	0.046	0.514	0.608	0.101	1.131	0.260	0.076	0.849	0.398
Right superior longitudinal fasciculus	0.022	0.244	0.807	0.019	0.207	0.836	0.053	0.588	0.558
Left sagittal stratum	0.197	2.232	0.027	− 0.034	− 0.372	0.711	0.091	1.014	0.313
Right sagittal stratum	0.202	2.284	0.024	0.058	0.647	0.519	− 0.043	− 0.475	0.636

Significance was defined as $p < 0.05$ (Bonferroni corrected for multiple comparisons) corresponding to $p < 0.00135$. p values meeting the significance criteria are bolded

time, resulting in opposite associations in adolescence and/or young adulthood. In the current study, differences between males and females did not change within the limited age range of our sample, though such effects during later infancy periods may exist in certain brain regions (Holland et al. 2014).

Patterns of sexual dimorphism suggest that processes underlying brain structure maturation differ between males and females. Many of the subcortical brain regions that differ between males and females contain significant populations of sex steroid receptors, including the amygdala, hippocampus, and basal ganglia (Lenroot and Giedd 2010).

As reviewed by Lenroot and Giedd (2010), levels of sex steroids can influence the cortical and subcortical structure and organization of the brain throughout childhood and adolescence. White matter differences between males and females are hypothesized to result from differences in myelin characteristics (Paus and Toro 2009), while quantitative MRI techniques sensitive to changes in myelin have suggested such differences are present during early brain development (Perrin et al. 2009; Deoni et al. 2011; Lebel et al. 2012; Dean et al. 2014c; Simmonds et al. 2014).

Brain volume relations with age

Volumetric measurements for total brain, gray matter, and white matter indicated age changes during the first month of life and reflect patterns in brain development that occur early in life (Gilmore et al. 2007, 2012; Knickmeyer et al. 2008; Makropoulos et al. 2014; Holland et al. 2014). Similarly, we observed age-related changes across both subcortical gray matter and white matter regions (Table 4), with the pallidum, left anterior cingulate gyrus, and posterior cingulate gyrus the only gray matter regions not exhibiting a significant age-relationship. These results complement previous studies of infant brain development showing that gray matter undergoes rapid maturation during the first weeks of postnatal development (Gilmore et al. 2007; Makropoulos et al. 2014; Holland et al. 2014), before continuing in a more linear fashion into adolescence and early adulthood (Giedd and Rapoport 2010).

White matter, on the other hand, develops at a slower rate during the first few weeks of life before experiencing significant increases later in infancy and throughout the lifespan (Barkovich et al. 1988; Paus et al. 2001; Bartzokis 2004; Huang et al. 2006). Volumes of the corpus callosum, bilateral posterior and left retrolenticular limbs of the internal capsule and the left-hemisphere sagittal stratum were significantly associated with infant gestational age. The corpus callosum and posterior limb of the internal capsule are some of the first white matter regions to mature (Paus et al. 2001; Deoni et al. 2012; Dubois et al. 2014), thus this significant age relationship may signify this early development. Furthermore, it is well-established that white matter develops along a posterior-to-anterior gradient (Paus et al. 2001; Deoni et al. 2012; Dean et al. 2014c, 2016; Dubois et al. 2014). Examining the internal capsules' slope estimates associated with the age (Table 4), we find the slopes of the posterior limb to be greater than that of the anterior limb, possibly representative of this posterior-to-anterior gradient of development. Similarly, the slopes of early developing white matter regions, including the corpus callosum and internal capsules, are observed to be greater than the slopes of white matter regions that develop later in childhood, such

as the superior longitudinal fasciculus and sagittal stratum; further indicating the developmental staging of white matter.

The observed age-related changes of subcortical gray matter volumes likely reflect critical neurodevelopmental processes. Mechanisms underlying early postnatal brain maturation, though intricate, are punctuated by the rapid and inter-related growth of synapses, dendrites, and fiber bundles. The density and complexity of the dendritic tree of neurons dramatically increases during the first months of postnatal development (Elston and Fujita 2014), while the development of new synapses (synaptogenesis) also begins around the time of birth and peak at various stages of development (Huttenlocher and Dabholkar 1997). Typical gray matter development follows an inverted U-shaped pattern, indicating that the cortex continues to develop through early adolescence before a pruning mechanism begins, at which point cortical volume decreases (Giedd et al. 1999; Durston et al. 2001; Casey et al. 2005; Giedd and Rapoport 2010). This reversal of white matter development occurs later in development; thus this pattern was not observed in the current study. Similar trajectories have been observed in other brain regions; however, the timing and rate of development varies between regions (Giedd et al. 1996, 1999; Gogtay and Thompson 2010; Giedd and Rapoport 2010). Cortical gray matter undergoes dynamic development along a posterior-anterior gradient (Gogtay et al. 2004), suggestive that brain regions responsible for higher-order cognitive functioning develop subsequent to the development of lower-order brain regions (Gogtay and Thompson 2010).

Similarly, the underlying mechanisms of white matter volume alterations may stem from changes in the fiber architecture as well as increases in myelination of neuronal pathways. Myelin maturation is a critical process that begins during the prenatal period and rapidly increases over the first 2 years of life before slowing and continuing throughout childhood, adolescence and early adulthood (Davison and Dobbing 1966; Yakovlev and Lecours 1967; Brody et al. 1987). Indeed, many recent neuroimaging studies utilizing quantitative techniques sensitive to developmental changes of white matter, such as myelination, have been conducted (Mukherjee et al. 2001, 2002; Dubois et al. 2006; Lebel et al. 2008, 2012; Lebel and Beaulieu 2011; Glasser and Van Essen 2011; Deoni et al. 2012, 2015; Kulikova et al. 2014; Dean et al. 2014b, c; Kunz et al. 2014; Chang et al. 2015; Croteau-Chonka et al. 2016). Myelination during early postnatal neurodevelopment affords the emergence and refinement of rapid and efficient inter-neuronal communication between brain regions, thus enabling advanced cognitive and behavioral functions (Fields 2005, 2008a, 2008b). Moreover, regional asymmetries may be explained, in part, by white matter differences and differences in myelination. While asymmetry of neuroanatomical features is a hallmark of human brain structure (Toga and Thompson 2003), the

rate and extent of myelination is modifiable through changes in inter-neuronal activity (Demerens et al. 1996; Fields 2015). Asymmetries in myelination may therefore reflect the formation of specialized neuronal networks and circuits (O'Muircheartaigh et al. 2013).

Findings from the current study shed light on ongoing structural processes during early brain maturation. However, they also raise important questions about the role underlying structural relations may have on the development of subsequent cognition and behavior. Moreover, it is possible that alterations in structural morphology make one vulnerable to later insults or psychopathology (Andersen 2003). For example, asymmetries of the amygdala are associated with differential processing of emotion, with the left hemisphere having a role in conscious emotional learning and the right hemisphere having a role in unconscious emotional learning (Morris et al. 1998; Davidson 2002, 2008; Lapate et al. 2016). Furthermore, increased amygdala volume has been consistently associated with psychopathology (Lupien et al. 2011; Davidson and McEwen 2012). While the structural asymmetries of amygdala volume we observed may be indicative of differential emotional processing in infants, systematic studies examining these relationships are required. However, the differential differences observed between males and females (i.e., decreased amygdalae volume found in females) could also imply that either sex may be inherently susceptible to developing psychopathology during periods of early brain development. Whether such critical or sensitive periods exist for such socio-emotional processes has not been thoroughly addressed. Future studies investigating relations between brain structural characteristics and the acquisition of specific cognitive and affective abilities and behaviors, will provide important understanding about these inter-dependent relationships. Such studies will also provide insight into mechanisms that make early neurodevelopment susceptible to both genetic and environmental forces.

This study has several limitations. First, the cross-sectional study design and restrictive age range of the sample limits the ability to examine individual developmental trajectories and rates of change. Examining these volumetric measures longitudinally would provide additional insight into the rapid changes occurring throughout early postnatal development while also provide insight into the individual variation of regional brain maturation. Another potential limitation of the current study is the region-of-interest analysis that was adopted. While this analysis approach was taken to examine the development and underlying relations of specific anatomic brain regions, this approach relies upon an accurate segmentation of each ROI. In particular, while atlas-based segmentation methods, as performed in this study, are common (Cabezas et al. 2011), these methods rely on an accurate registration between the individual subject and atlas. Here, we used atlases that were constructed from a

similar age-group as the current study (Shi et al. 2011; Oishi et al. 2011), as well as state-of-the-art algorithms (Avants et al. 2011a) to register subject data to the template. Still, additional segmentation techniques, such as multi-atlas or probabilistic segmentation methods, may provide additional benefits (Cabezas et al. 2011). Future work comparing atlas-based segmentation methods to these alternative algorithms in infant populations is of interest. Voxel-based methods, such as voxel-based morphometry or tensor-based morphometry, to examine brain structure may be informative about subtle developmental associations in the 1-month-infant brain; however, discrepancies with these methods can be confounded by small errors in masking and spatial normalization. Follow-up voxel-based analyses will, however, allow us to examine subtler developmental asymmetries or sexual dimorphisms that are present or begin to emerge during early postnatal maturation.

Conclusion

In this work, we examined regional brain structures in the 1-month infant. We observed that measures of subcortical brain volume relate to gestational corrected age and revealed patterns of regional asymmetry and sexual dimorphism. Though total brain volume was associated with commonly utilized newborn growth measures, the majority of subcortical brain regions were not associated with such measures. Our results herein complement and add to a growing corpus of work investigating early neurodevelopment. Follow-up investigations of this sample will provide important insights into the longitudinal mechanisms of postnatal brain maturation.

References

Allen JS, Damasio H, Grabowski TJ et al (2003) Sexual dimorphism and asymmetries in the gray-white composition of the human cerebrum. Neuroimage 18:880–894

Andersen SL (2003) Trajectories of brain development: point of vulnerability or window of opportunity? Neurosci Biobehav Rev 27:3–18

Avants BB, Tustison NJ, Song G et al (2011a) A reproducible evaluation of ANTs similarity metric performance in brain image registration. Neuroimage 54:2033–2044

Avants BB, Tustison NJ, Wu J et al (2011b) An open source multivariate framework for n-tissue segmentation with evaluation on public data. Neuroinformatics 9:381–400

Barkovich AJ, Kjos BO, Jackson DE, Norman D (1988) Normal maturation of the neonatal and infant brain: MR imaging at 1.5 T. Radiology 166:173–180

Bartzokis G (2004) Quadratic trajectories of brain myelin content: unifying construct for neuropsychiatric disorders. Neurobiol Aging 25:49–62

Belmonte MK, Allen G, Beckel-Mitchener A et al (2004) Autism and abnormal development of brain connectivity. J Neurosci 24:9228–9231

Brody BA, Kinney HC, Kloman AS, Gilles FH (1987) Sequence of central nervous system myelination in human infancy. I. An autopsy study of myelination. J Neuropathol Exp Neurol 46:283–301

Cabezas M, Oliver A, Lladó X et al (2011) A review of atlas-based segmentation for magnetic resonance brain images. Comput Meth Prog Bio 104:e158–e177

Casey BJ, Tottenham N, Liston C, Durston S (2005) Imaging the developing brain: what have we learned about cognitive development? Trends Cogn Sci 9:104–110

Caviness VS Jr, Kennedy DN, Richelme C et al (1996) The human brain age 7–11 years: a volumetric analysis based on magnetic resonance images. Cereb Cortex 6:726–736

Chang YS, Owen JP, Pojman NJ et al (2015) White matter changes of neurite density and fiber orientation dispersion during human brain maturation. PLoS One 10:e0123656

Courchesne E, Pierce K (2005) Brain overgrowth in autism during a critical time in development: implications for frontal pyramidal neuron and interneuron development and connectivity. Int J Dev Neurosci 23:153–170

Courchesne E, Chisum HJ, Townsend J et al (2000) Normal brain development and aging: quantitative analysis at in vivo MR imaging in healthy volunteers. Radiology:672–682

Croteau-Chonka EC, Dean DC, Remer J et al (2016) Examining the relationships between cortical maturation and white matter myelination throughout early childhood. Neuroimage 125:413–421

Davidson RJ (2002) Anxiety and affective style: role of prefrontal cortex and amygdala. Biol Psychiatry 51:68–80

Davidson RJ (2008) Cerebral asymmetry and emotion: conceptual and methodological conundrums. Cogn Emot 7:115–138

Davidson RJ, McEwen BS (2012) Social influences on neuroplasticity: stress and interventions to promote well-being. Nat Neurosci 15:689–695

Davison AN, Dobbing J (1966) Myelination as a vulnerable period in brain development. Br Med Bull 22:40–44

Dean DC III, Dirks H, O'Muircheartaigh J et al (2014a) Pediatric neuroimaging using magnetic resonance imaging during non-sedated sleep. Pediatr Radiol 44:64–72

Dean DC III, O'Muircheartaigh J, Dirks H et al (2014b) Modeling healthy male white matter and myelin development: 3 through 60 months of age. Neuroimage 84:742–752

Dean DC III, O'Muircheartaigh J, Dirks H et al (2014c) Characterizing longitudinal white matter development during early childhood. Brain Struct Funct:1921–1931

Dean DC III, O'Muircheartaigh J, Dirks H et al (2016) Mapping an index of the myelin g-ratio in infants using magnetic resonance imaging. Neuroimage 132:225–237

Dean DC III, Planalp EM, Wooten W et al (2017) Mapping white matter microstructure in the one month human brain. Sci Rep 7(1):9759

Dehaene-Lambertz G, Hertz-Pannier L, Dubois J (2006) Nature and nurture in language acquisition: anatomical and functional brain-imaging studies in infants. Trends Neurosci 29:367–373

Demerens C, Stankoff B, Logak M et al (1996) Induction of myelination in the central nervous system by electrical activity. PNAS 93:9887–9892

Deoni SCL, Mercure E, Blasi A et al (2011) Mapping infant brain myelination with magnetic resonance imaging. J Neurosci 31:784–791. https://doi.org/10.1523/JNEUROSCI.2106-10.2011

Deoni SCL, Dean DC, O'Muircheartaigh J et al (2012) Investigating white matter development in infancy and early childhood using myelin water faction and relaxation time mapping. Neuroimage 63:1038–1053

Deoni SCL, Dean DC, Remer J et al (2015) Cortical maturation and myelination in healthy toddlers and young children. Neuroimage 115:147–161

DiCicco-Bloom E, Lord C, Zwaigenbaum L et al (2006) The developmental neurobiology of autism spectrum disorder. J Neurosci 26:6897–6906

Dobbing J (1990) Vulnerable periods in developing brain. In: Commentary. Springer, London, pp 1–17

Dubois J, Hertz-Pannier L, Dehaene-Lambertz G et al (2006) Assessment of the early organization and maturation of infants' cerebral white matter fiber bundles: a feasibility study using quantitative diffusion tensor imaging and tractography. Neuroimage 30:1121–1132

Dubois J, Hertz-Pannier L, Cachia A et al (2009) Structural asymmetries in the infant language and sensor–motor networks. Cereb Cortex 19:414–423

Dubois J, Dehaene-Lambertz G, Kulikova S et al (2014) The early development of brain white matter: a review of imaging studies in fetuses, newborns and infants. Neuroscience 276:48–71

Durston S, Hulshoff Pol HE, Casey BJ et al (2001) Anatomical MRI of the developing human brain: what have we learned? J Am Acad Child Adolesc Psychiatry 40:1012–1020

Elston GN, Fujita I (2014) Pyramidal cell development: postnatal spinogenesis, dendritic growth, axon growth, and electrophysiology. Front Neuroanat 8:13644

Evans AC, Brain Development Cooperative Group (2006) The NIH MRI study of normal brain development. Neuroimage 30:184–202

Fields RD (2005) Myelination: an overlooked mechanism of synaptic plasticity? Neuroscientist 11:528–531

Fields RD (2008a) White matter matters. Sci Am 298:54–61

Fields RD (2008b) White matter in learning, cognition and psychiatric disorders. Trends Neurosci 31:361–370

Fields RD (2015) A new mechanism of nervous system plasticity: activity-dependent myelination. Nat Rev Neurosci 16:756–767

Giedd JN, Rapoport JL (2010) Structural MRI of pediatric brain development: what have we learned and where are we going? Neuron 67:728–734

Giedd JN, Snell JW, Lange N et al (1996) Quantitative magnetic resonance imaging of human brain development: ages 4–18. Cereb Cortex 6:551–559

Giedd JN, Blumenthal J, Jeffries NO et al (1999) Brain development during childhood and adolescence: a longitudinal MRI study. Nat Neurosci 2:861–863

Gilmore JH, Lin W, Prastawa MW et al (2007) Regional gray matter growth, sexual dimorphism, and cerebral asymmetry in the neonatal brain. J Neurosci 27:1255–1260

Gilmore JH, Shi F, Woolson SL et al (2012) Longitudinal development of cortical and subcortical gray matter from birth to 2 years. Cereb Cortex 22:2478–2485

Glasser MF, Van Essen DC (2011) Mapping Human cortical areas in vivo based on myelin content as revealed by T1- and T2-weighted MRI. J Neurosci 31:11597–11616

Gogtay N, Thompson PM (2010) Mapping gray matter development: implications for typical development and vulnerability to psychopathology. Brain Cogn 72:6–15

Gogtay N, Giedd JN, Lusk L et al (2004) Dynamic mapping of human cortical development during childhood through early adulthood. PNAS 101:8174–8179

Goldstein JM, Seidman LJ, Horton NJ et al (2001) Normal sexual dimorphism of the adult human brain assessed by in vivo magnetic resonance imaging. Cereb Cortex 11:490–497

Hill J, Dierker D, Neil J et al (2010) A surface-based analysis of hemispheric asymmetries and folding of cerebral cortex in term-born human infants. J Neurosci 30:2268–2276

Holland D, Chang L, Ernst TM et al (2014) Structural growth trajectories and rates of change in the first 3 months of infant brain development. JAMA Neurol 71:1266–1274

Huang H, Zhang J, Wakana S et al (2006) White and gray matter development in human fetal, newborn and pediatric brains. Neuroimage 33:27–38

Hugdahl K, Davidson RJ (2004) The asymmetrical brain. MIT Press, London

Hüppi PS, Maier SE, Peled S et al (1998a) Microstructural development of human newborn cerebral white matter assessed in vivo by diffusion tensor magnetic resonance imaging. Pediatr Res 44:584–590

Hüppi PS, Warfield S, Kikinis R et al (1998b) Quantitative magnetic resonance imaging of brain development in premature and mature newborns. Ann Neurol 43:224–235

Huttenlocher PR, Dabholkar AS (1997) Regional differences in synaptogenesis in human cerebral cortex. J Comp Neurol 387:167–178

Knickmeyer RC, Gouttard S, Kang C et al (2008) A structural MRI study of human brain development from birth to 2 years. J Neurosci 28:12176–12182

Kolb B, Gibb R (2011) Brain plasticity and behaviour in the developing brain. J Can Acad Child Adolesc Psychiatry 20:265–276

Koolschijn PCMP., Crone EA (2013) Sex differences and structural brain maturation from childhood to early adulthood. Dev Cogn Neurosci 5:106–118

Kulikova S, Hertz-Pannier L, Dehaene-Lambertz G et al (2014) Multiparametric evaluation of the white matter maturation. Brain Struct Funct 1–16

Kunz N, Zhang H, Vasung L et al (2014) Assessing white matter microstructure of the newborn with multi-shell diffusion MRI and biophysical compartment models. Neuroimage 96:288–299

Lapate RC, Rokers B, Tromp DPM et al (2016) Awareness of emotional stimuli determines the behavioral consequences of amygdala activation and amygdala-prefrontal connectivity. Sci Rep 6:25826

Lebel C, Beaulieu C (2011) Longitudinal development of human brain wiring continues from childhood into adulthood. J Neurosci 31:10937–10947

Lebel C, Walker L, Leemans A et al (2008) Microstructural maturation of the human brain from childhood to adulthood. Neuroimage 40:1044–1055

Lebel C, Gee M, Camicioli R et al (2012) Diffusion tensor imaging of white matter tract evolution over the lifespan. Neuroimage 60:340–352

Lenroot RK, Giedd JN (2010) Sex differences in the adolescent brain. Brain Cogn 72:46–55

Lenroot RK, Gogtay N, Greenstein DK et al (2007) Sexual dimorphism of brain developmental trajectories during childhood and adolescence. Neuroimage 36:1065–1073

Lupien SJ, Parent S, Evans AC et al (2011) Larger amygdala but no change in hippocampal volume in 10-year-old children exposed to maternal depressive symptomatology since birth. Proc Natl Acad Sci USA 108:14324–14329

Makki MI, Hagmann C (2017) Regional differences in interhemispheric structural fibers in healthy, term infants. J Neurosci Res 95:876–884

Makropoulos A, Gousias IS, Ledig C et al (2014) Automatic whole brain MRI segmentation of the developing neonatal brain. IEEE Trans Med Imaging 33:1818–1831

Makropoulos A, Aljabar P, Wright R et al (2016) Regional growth and atlasing of the developing human brain. Neuroimage 125:456–478

Morris JS, Öhman A, Dolan RJ (1998) Conscious and unconscious emotional learning in the human amygdala. Nature 393:467–470

Mukherjee P, Miller JH, Shimony JS et al (2001) Normal brain maturation during childhood: developmental trends characterized with diffusion-tensor MR imaging. Radiology 221:349–358

Mukherjee P, Miller JH, Shimony JS et al (2002) Diffusion-tensor MR imaging of gray and white matter development during normal human brain maturation. AJNR Am J Neuroradiol 23:1445–1456

O'Muircheartaigh J, Dean DC III, Dirks H et al (2013) Interactions between white matter asymmetry and language during neurodevelopment. J Neurosci 33:16170–16177

Oishi K, Mori S, Donohue PK et al (2011) Multi-contrast human neonatal brain atlas: application to normal neonate development analysis. Neuroimage 56:8–20

Paus T, Toro R (2009) Could sex differences in white matter be explained by g ratio? Front Neuroanat 3:14

Paus T, Collins DL, Evans AC et al (2001) Maturation of white matter in the human brain: a review of magnetic resonance studies. Brain Res Bull 54:255–266

Perrin JS, Leonard G, Perron M et al (2009) Sex differences in the growth of white matter during adolescence. Neuroimage 45:1055–1066

Pfefferbaum A, Mathalon DH, Sullivan EV et al (1994) A quantitative magnetic resonance imaging study of changes in brain morphology from infancy to late adulthood. Arch Neurol 51:874–887

R Development Team (2014) R: a language and environment for statistical computing. R Foundation for Statistical Computing, Vienna

Reiss AL, Abrams MT, Singer HS et al (1996) Brain development, gender and IQ in children. A volumetric imaging study. Brain 119(Pt 5):1763–1774

Shi F, Yap P-T, Wu G et al (2011) Infant brain atlases from neonates to 1- and 2-year-olds. 6:e18746–e18711

Simmonds DJ, Hallquist MN, Asato M, Luna B (2014) Developmental stages and sex differences of white matter and behavioral development through adolescence: a longitudinal diffusion tensor imaging (DTI) study. Neuroimage 92:356–368

Stiles J, Jernigan TL (2010) The basics of brain development. Neuropsychol Rev 20:327–348

Toga AW, Thompson PM (2003) Mapping brain asymmetry. Nat Rev Neurosci 4:37–48

Wilke M, Krägeloh-Mann I, Holland SK (2007) Global and local development of gray and white matter volume in normal children and adolescents. Exp Brain Res 178:296–307

Yakovlev P, Lecours IR (1967) Regional development of the brain in early life. Minkowski A

Zhang Y, Brady M, Smith S (2001) Segmentation of brain MR images through a hidden Markov random field model and the expectation-maximization algorithm. Med Imaging IEEE Trans 20:45–57